Multiple Structural Alignment by Secondary Structures: Algorithm and Applications

Oranit Dror[1]*, Hadar Benyamini[2], Ruth Nussinov[2,3]†, Haim J. Wolfson[1]

[1] School of Computer Science, Raymond and Beverly Sackler Faculty of Exact Sciences,
Tel Aviv University, Tel Aviv 69978, Israel,
Telefax : +972-3-640 6476, e-mail : {oranit,wolfson}@post.tau.ac.il.

[2] Sackler Inst. of Molecular Medicine, Sackler Faculty of Medicine
Tel Aviv University, Tel Aviv 69978, Israel.

[3] Basic Research Program, SAIC-Frederick, Inc,
Lab. of Experimental and Computational Biology, NCI - FCRDC,
Bldg 469, Rm 151, Frederick, MD 21702, USA.

Running Title: Multiple Structural Alignment
Text Format: LaTex, Word
Number of pages: 44, **Number of figures:** 11, **Number of tables:** 4

*To whom correspondence should be addressed, email: oranit@post.tau.ac.il.

 Funded in part by the NCI under contract NO1-CO-12400.

Abstract

We present MASS (**M**ultiple **A**lignment by **S**econdary **S**tructures), a novel, highly efficient method for structural alignment of multiple protein molecules and detection of common structural motifs. MASS is based on a two-level alignment, using both secondary structure and atomic representation. Utilizing secondary structure information aids in filtering out noisy solutions and achieves efficiency and robustness.

Currently, only a few methods are available for addressing the multiple structural alignment task. In addition to using secondary structure information, the advantage of MASS as compared to these methods is that it is a combination of several important characteristics: (i) while most existing methods are based on series of pairwise comparisons, and thus might miss optimal global solutions, MASS is truly multiple, considering all the molecules simultaneously; (ii) MASS is sequence order independent and thus capable of detecting non-topological structural motifs; (iii) MASS is able to detect not only structural motifs, shared by all input molecules, but also motifs shared only by subsets of the molecules.

Here, we show the application of MASS to various protein ensembles. We demonstrate its ability to handle a large number (order of tens) of molecules, to detect non-topological motifs and to find biologically meaningful alignments within non predefined subsets of the input. In particular, we show how by using conserved structural motifs, detected by MASS, one can guide protein-protein docking, which is a notoriously difficult problem.

Availability. MASS is freely available on `http://bioinfo3d.cs.tau.ac.il/MASS`

Keywords. Multiple structural comparison, Non-sequential alignment, Non-topological motif, Supersecondary structural motif, Docking, Protein structure classification, Large-scale structure comparison

The motivation for enhanced efficient structural alignment methods is quite obvious. It is well established that the function of a protein may be inferred from its 3D structure (Branden & Tooze, 1999). Thus, structural homology may imply a similar function. This observation gave rise to the development of structural alignment tools, which are becoming increasingly useful upon the acceleration of protein structure determination and the Structural Genomics project. Structural alignment is a key tool for protein classification, evolutionary relationship studies and structure prediction using homology modelling or threading.

Many methods have been developed to address the *pairwise structural alignment* task. See (Brown *et al.*, 1996; Lemmen & Lengauer, 2000; Eidhammer *et al.*, 2001) for comprehensive reviews . In contrast, only a few methods are available for aligning multiple structures. However, it is clear that multiple alignment carries significantly more information and thus is a much more powerful tool.

Most of the currently available methods for multiple structural alignment are pairwise-based. They find common substructures through a series of comparisons between pairs of molecules. These methods combine a pairwise structural alignment and a heuristic to merge pairwise alignments into a multiple alignment, e.g. the *center-star* and the *progressive tree* approaches that are widely used in multiple-sequence alignment (Gusfield, 1993). A representative example is the method of Gerstein and Levitt. In this approach a central structure is defined as the structure that on average is closest to all other structures. Then, a multiple alignment is constructed based on aligning the remaining structures to the central structure (Gerstein & Levitt, 1996). Other well-known methods of this type are SSAPm (Taylor *et al.*, 1994), PrISM (Yang & Honig, 2000*b*), STAMP (Russell & Barton, 1992), (Sali & Blundell, 1990), (Ding *et al.*, 1994), (May & Johnson, 1995), (Akutsu & Sim, 1999) and (Guda *et al.*, 2001).

The pairwise-based methods have the limitation that in each pairwise alignment the only available information is about the two molecules involved. Thus, alignments that are optimal for the whole input set might be missed, if they are not also optimal for every pair (Eidhammer *et al.*, 2001). Our method, MASS, is truly multiple. It considers all the given structures simultaneously, rather than starting from pairwise alignments. Three other truly-multiple methods are (Escalier *et al.*, 1988), MUSTA (Leibowitz *et al.*, 2001*a*; Leibowitz *et al.*, 2001*b*) and MultiProt (Shatsky *et al.*, 2002). The algorithm of Escalier et al. recursively finds common substructures of increasing size. It combines two common sets of k atoms to build a common set of $k + 1$ atoms. MUSTA employs *Geometric Hashing* (Lamdan & Wolfson, 1988; Nussinov & Wolfson, 1991) to find sets of k atoms, common to the *all* input molecules, and then extends them into global common substructures. MultiProt is based on short polypeptide fragment alignments. It detects structurally similar common pieces, which are then extended to compute global alignments.

MASS is based on a two-level alignment, using both secondary structure and atomic representation. The rationale behind this approach is that proteins are inherently composed of secondary structure elements (SSEs). These are the regions within a protein that provide its stabilizing scaffold, onto which the functional sites are grafted. Consequently, SSEs are evolutionarily highly conserved while mutations frequently occur at flexible loops, which are more difficult to align. Indeed, SSE representation has been successfully used in several algorithms for pairwise alignment and database searching (Mitchel *et al.*, 1989; Grindley

et al., 1993; Holm & Sander, 1995; Koch *et al.*, 1996; Alesker *et al.*, 1996; Alexandrov & Fischer, 1996; Lu, 2000; Yang & Honig, 2000*a*).

Structural description at the secondary structure level conveys both efficiency and accuracy: (i) *Efficiency* - The average number of SSEs in a globular protein (~ 15) is smaller by tenfold compared to the average number of residues (~ 300). Representing proteins by their SSEs introduces great savings in structural description, compared to residue or atomic representation. As a result, protein structures can be treated more easily and significant improvement in computation can be achieved, especially when many structures are analyzed; (ii) *Accuracy and noise filtering* - Due to the high atom density in protein molecules, any random pair of proteins can be superimposed so that many of their atoms are aligned. However, such an alignment is most probably biologically irrelevant. An SSE-based method avoids this problem and is more likely to detect a motif of biological value, like a fold fingerprint or a common binding site.

The majority of the methods for multiple structure alignment use *dynamic programming* (Needleman & Wunsch, 1970). As a result they have the disadvantage of being dependent on the sequence order of the polypeptide chain. MASS is a sequence-order independent method [1]. Thus, it can find non-topological alignments. Such a capability is essential for detecting common structural motifs that exist due to convergent evolution, but with no fold homology. In certain cases, where order dependency is preferred, there is also an option in MASS to consider the order of the protein amino acids. This option can be used to cluster topologically similar proteins or to obtain a structure-based sequence alignment.

Another important feature of MASS is the ability to detect *subset alignments*. In addition to finding structural motifs shared by the *whole* given set of molecules, MASS detects motifs shared by non-predefined subsets. This capability prevents the loss of good alignments due to structural outliers and is highly useful in protein classification of heterogenous ensembles.

Here we describe the application of MASS to several types of protein ensembles. We demonstrate that MASS successfully handles difficult cases of multiple structural alignment. These include aligning large-scale protein ensembles (on the order of tens of proteins), detection of non-topological structural motifs, and detection of subset alignments, which is very useful for protein structural classification. We further show how focusing on structurally conserved motifs significantly improves the performance of protein-protein docking, suggesting such an approach as a viable strategy in this extremely difficult problem.

1 Algorithm

Our goal is to detect structural motifs that are common to a group of proteins. This requirement is more complicated than it appears at first sight. We would like the algorithm to address the following questions: (i) Does the whole input set of proteins share any structural similarity? If so, what is the largest common substructure? (ii) Are there additional significant common motifs, apart from the largest one? (iii) Are there structural motifs that are shared by only a subset of the input proteins?

[1] In the first stage, MASS disregards the order of the SSEs along the polypeptide chain. In the second stage, the backbone order of all C_α atoms is ignored

Below we will give a more formal statement of the problem, followed by a description of the MASS algorithm. A more detailed technical description followed by a comprehensive runtime complexity analysis can be found in (Dror *et al.*, 2003).

1.1 Problem Statement

If we represent a protein structure as a set of points in 3D space, where each point is the center of a C_α atom, then the problem can be thought of as a variant of the *largest common point set* (LCP) problem. In this problem we are given a collection of m sets of 3D points and the task is to detect the largest point set of which a congruent copy appears in *each* of the input sets. Unfortunately, this problem is known to be NP-hard (Akutsu & Halldorsson, 2000).

The LCP formulation above is not suitable for practical applications. It assumes that the positions of all atoms are known precisely and searches for an exact alignment between common substructures. However, for molecular structures, atom positions are not known exactly and an exact alignment may be impossible to find. Therefore, it is more practical to detect the largest point set of which an *almost-congruent* copy appears in each of the input sets. Two point-sets are said to be almost-congruent if the distance between them is below a predefined threshold. One of the most commonly used distance functions is the *Root Mean Square Deviation* (RMSD) (Kaindl & Steipe, 1997).

We actually wish to address an even more complicated task. A biologically meaningful motif might not be the largest common substructure. Thus, one will be interested to find smaller common substructures as well. However, in practice there is no need to detect all possible common substructures. A better approach is to detect the r largest ones or all common substructures above a certain size.

The task is further complicated by the requirement to detect not only substructures common to the *whole* given set of molecules, but also substructures shared by non-predefined subsets of the input molecules (*subset alignments*). This requirement complicates the problem since the number of subsets is exponential in the number of the input molecules. In addition, the goal should be redefined. It may be impractical to supply the end-user all common substructures for each possible subset of the input molecules. Even outputting just the largest common substructure for each subset may be infeasible. It is better to rank the solutions according to some scoring function and to output the highest scoring ones. However, no one specific scoring function fits all. The reason is that several trade-offs exist, e.g. (i) number of aligned molecules vs. core size; and (ii) core size vs. the size of the smallest participating molecule. An explanation of how these trade-offs are addressed in MASS is given below.

Below we propose a heuristic algorithm for solving this hard problem. The algorithm runs in polynomial time and yields good results.

1.2 Algorithm Outline

As was discussed in section 1.1, the problem that we are trying to solve is NP-hard. Therefore, to reduce the runtime complexity we exploit the fact that the structures to be compared are not mere point sets in 3D space, but protein structures. Protein structures are composed of secondary structure elements (SSEs). The number of SSEs in a protein is smaller by tenfold compared to the number of residues. Thus, structural description at the secondary structure level is significantly reduced compared to the C_α-atomic level, and can lead to considerable savings in computation, especially when many structures are analyzed.

The algorithm is based on a two-level alignment, using both secondary structure and atomic representation (see Figure 1). In the first stage, the protein structures are represented by their SSEs. We assume that a structural alignment is biologically interesting only if its core consists of at least two SSEs. This assumption is based on the definition of a structural motif (Lehninger *et al.*, 1993). According to this assumption, pairs of SSEs which are conserved in at least two proteins are detected and initial local alignments are obtained. In the second stage, we use the C_α atomic coordinates of the protein structures to refine and extend the initial alignments, in order to obtain global atomic superpositions.

• **Input.** The input for the method is a collection of m proteins: $P_1, P_2, ..., P_m$. For each protein two inputs are given: (i) the 3D coordinates of its atoms in PDB format (Berman *et al.*, 2000); and (ii) the assignment of SSE types to its residues. In the current implementation of MASS, three types of SSE assignment are supported: PDB (Berman *et al.*, 2000), DSSP (Kabsch & Sander, 1983) and DSSPcont (**?**).

• **Representing Secondary Structure Elements.** The SSEs that we base our alignments on are helices and strands, where all types of helices (e.g. α, π, $3-10$) are grouped together in one category.

We represent each SSE by its axis (see Figure 2). The axis of an SSE is a directed 3D line segment, defined as follows: (i) it is located on the *least squares line* of all the α-carbon atoms of the SSE, i.e. the line that minimizes the sum of squares of the perpendicular distances from the α-carbon atoms to the line; (ii) its length is the distance between the two projection points of the terminal α-carbon atoms of the SSE; and (iii) its direction is along the polypeptide chain.

• **Detecting Multiple Base Alignments.** A *basis* is defined as an ordered pair of SSEs. Based on the assumption that the core of an interesting alignment consists of at least two SSEs, our purpose in this stage is to find almost-congruent bases that appear in several proteins (in at least two by default). To find such bases in an efficient manner, we employ the *Geometric Hashing* paradigm (Nussinov & Wolfson, 1991). Specifically, we represent each basis by a 5D vector, termed *fingerprint*. The fingerprint is invariant to a 3D rotation and translation and composed of the following five components (see Figure 3a): (i) the type of the first SSE; (ii) the type of the second SSE; (iii) the angle between their axial vectors; (iv) the midpoint-to-midpoint distance between their axes; and (v) their line distance, i.e. the closest distance in space between their (infinite) least-squares lines.

We store the bases of all proteins in a 5D grid addressed by their fingerprint. Congruent bases have the same fingerprint and thus are stored in the same grid bin. Almost-congruent bases have similar fingerprints and thus reside close to each other in the grid, but not necessarily in the same bin. The resolution of the grid is determined by the tolerance that we allow between the fingerprints of bases we consider as almost congruent. By default two bases are considered to be almost-congruent if: (i) the types of their SSEs are the same; (ii) the difference between their midpoint-to-midpoint and line distances is up to 1.5 Å; and (iii) the difference between their angles is up to 0.3 radians. These values have been determined empirically.

We then iterate over the grid bins. For each bin, we extract all the bases of the bin and of adjacent bins and group them together in the same *Base Bucket* (see Figure 3b). A base bucket is simply a container that stores bases in columns according to the protein they belong to. Bases derived from the same protein are stored in the same column.

Almost-congruent bases are stored in the same base bucket. A collection of almost-congruent bases, each belonging to a different column (i.e. protein) of a base bucket, induces a local multiple alignment between the respective proteins, whose core consists of at least two SSEs. Specifically, one basis is selected as a *pivot* and the rest of the bases are superimposed on it. The obtained vector of pairwise alignments defines a local multiple alignment between the respective proteins and is termed *multiple base alignment*. The core of this alignment consists of at least two SSEs, but can be extended into a larger substructure. Note that the selection of the pivot may influence the alignment. Thus, so as not to be influenced, there is an option in MASS to iteratively choose each basis to be a pivot.

A multiple alignment is defined by an underlying set of pairwise alignments. Thus, as a first step in evaluating the possible multiple base alignments, we compute their pairwise alignment components. Specifically, for each base bucket we compute all the alignments between two bases, taken from two different columns.

Two ways for aligning a pair of bases are supported. In the first approach we represent each SSE by the list of its C_α atoms. Then, we find the transformation between the two bases that aligns the maximal number of atoms with the minimal RMSD. In the second approach we uniquely define a cartesian reference frame for each basis. Then, we superimpose the two reference frames one onto another. This approach is less accurate than the former. However, it is useful in cases in which the atomic coordinates of the proteins are not known and the only available data are about their secondary structure, for instance information extracted from models or EM density maps (Chiu *et al.*, 2002).

• **Clustering.** Assume we have a pair of proteins whose largest common substructure consists of more than two SSEs. For such a pair, we may get several local base alignments (one alignment for each basis in their common substructure). These alignments have almost the same transformation, but a different local SSE core. Our aim at this stage is to cluster all the local base alignments in order to find the ones with similar transformations and merge them into a new global alignment. The match list of the new global alignment is the union of the original local match lists and its transformation is the one that aligns the SSEs of the new match list with minimum RMSD (computed by the *Least-Squares Fitting* method (Kabsch, 1978)).

• **Global Extension.** After the clustering, the core of each pairwise alignment is a set of SSEs. In this stage, we extend the cores of these alignments by detecting corresponding C_α-atoms, which do not necessarily belong to SSEs. Each pairwise alignment is associated with a transformation. This transformation takes two sets of SSEs, one from each protein, and superimposes the second set onto the first set (i.e. the one from the pivot protein). We apply this transformation on the second protein, so that it is fully superimposed onto the pivot protein. We then detect in linear time pairs of C_α atoms, one atom from each protein, whose positions are close enough (Bachar *et al.*, 1993). These atom pairs are added to the alignment's match list. The transformation of the alignment is then refined by employing the *Least-Squares Fitting* method (Kabsch, 1978).

• **Computing the Best Global Multiple Alignments.** What are the best global multiple alignments? There is no absolute answer to this question. As was mentioned above, there are several trade-offs, e.g.: (i) number of aligned molecules vs. core size; and (ii) core size vs. the size of the smallest participating molecule. The trade-offs are derived from the fact that we compare subset alignments with different participating molecules. Two approaches for addressing the first trade-off have been implemented: (i) The score of an alignment is defined as a function of the number of participating molecules (k) and the core size (l): $F(k,l) = l \cdot \binom{k}{2}$; (ii) Providing the alignments with the largest cores for each possible number of aligned molecules. The second trade-off is addressed by using a *relative* scoring function, which rewards alignments with a high ratio between the core size and the size of the smallest participating molecule. The choice of the scoring function depends on the input and thus is a user-defined parameter.

As was discussed before, the number of possible multiple alignments defined by the base buckets is exponential in the number of input molecules. Our aim at this stage is not to compute all of them, but to suggest a heuristic solution for choosing and computing only the best ones. For each base bucket we compute the set of best multiple alignments over its columns. We select each basis as a pivot and choose at most one basis from each of the remaining columns in an iterative manner. The chosen bases are the ones that yield the best global alignment. The core of the resulting multiple alignment is the intersection of the cores of the underlying pairwise alignments. Since we construct only one multiple alignment for each basis, the number of alignments is polynomial in the number of bases.

1.3 Complexity

The overall runtime complexity of the algorithm is bounded by $O(m^2 s^4 (s^4 \log s + n))$, where m is the number of input proteins and s and n are the maximum number of SSEs and residues found in each protein respectively[2] (Dror *et al.*, 2003). This is the worst case complexity, when all the bases of all proteins are stored in one base bucket. The actual number of bases of a bucket is influenced by two factors: (i) the number of recurring motifs in each protein; and (ii) the structural variance among the input proteins. The former influences the number of bases of a protein that will reside in the same base bucket. The latter influences the number of occupied bucket's columns. Since not all the bases of a protein are almost-congruent,

[2]Note that in a typical globular protein $s \sim 15$ and $n \sim 300$

there will be fewer bases in each bucket's column. Furthermore, when the input proteins are less structurally similar, fewer bases of them will be in the same base buckets, so there will be less than m occupied columns. To estimate the 'practical' runtime complexity, we have conducted a set of experiments. The behavior of the complexity in these tests was quadratic in both the number of molecules (m) and SSEs (s). This is much lower than the theoretical complexity.

2 Results and Discussion

We have conducted numerous experiments with the MASS program. Here we describe some of these, demonstrating the capability of MASS to address challenging cases of multiple structural alignment. These cases include: (i) detection of subset alignments and their use for structural classification; (ii) detection of non-topological alignments; (iii) detection of more than one common substructure for a given set of molecules; and (iv) alignments of large-scale ensembles. Finally, we demonstrate how by utilizing structural conservation information, we are able to improve protein-protein docking. Additional examples for multiple alignments obtained by MASS can be found in (Dror *et al.*, 2003).

All experiments were performed on a standard PC workstation (Pentium© 4 1800 MHz processor with 1GB internal memory). Secondary structure assignment in all experiments was determined by the DSSP program (Kabsch & Sander, 1983). The PDB codes of the discussed ensembles are listed in Table 4.

2.1 Detection of Subset Alignments for Structural Classification

Here we show that MASS is capable of detecting not only structural motifs common to the whole given set of molecules, but also motifs shared only by a subset of molecules. We further show that such a capability may be very useful for structural classification.

• **CL-GL Ensemble.** We have used MASS to align a set of twelve sequentially non-redundant structures taken from the 'Actin depolymerizing proteins' fold of the SCOP database (Murzin *et al.*, 1995). This fold contains only two families: the Cofilin-like (CL) and the Gelsolin-like (GL) families. The two families share a central five-stranded β-sheet of the form BACDE that is flanked between two α-helices: one long helix between strands D and E (α_1) and one short helix in the C terminus (α_2). The CL family has two additional α-helices: an N terminal helix and a short helix between strands B and C. The two families are related structurally but not sequentially (Hatanaka *et al.*, 1996; Benyamini *et al.*, 2003). The twelve-molecule ensemble contains four CL structures (PDB: 1f7s, 1ak6 ,1cfyB and 1cnu) and eight GL (PDB: 1d0nA:27-152, 1d0nA:153-262, 1d0nA:263-383, 1d0nA:384-532, 1d0nA:533-628, 1d0nA:629-755, 1svy and 2vik).

The running time of MASS on this ensemble was 36 seconds. Figure 4a presents the structural alignment of all twelve proteins. The common core consists of 28 residues with an RMSD of 1.9 Å. Strands A,C,D,E and helix α_1 are structurally conserved. Strand B is only

partially conserved due to a slight twist. Helix α_2 is not conserved, because its coordinates are missing in *arabidopsis thaliana* cofilin protein (PDB: 1f7s).

MASS also detected meaningful subset alignments. The graph in Figure 5 presents the maximal core size for every number of aligned molecules. As expected, the maximal core size decreases as the number of aligned molecules increases. However, the dependence is not linear: a significant decrease in the maximal core size is observed in the following three cases: (i) a decrease of 17 residues between three to four molecules; (ii) a decrease of 32 residues between four to five molecules; and (iii) a decrease of 15 residues between eight to nine molecules. The decrease in these cases indicates that the best subset alignments among eight, four and three molecules may be the most interesting ones. Indeed, the best alignment among eight molecules consists solely of the GL family members. Their common core consists of 63 residues with an RMSD of 1.5 Å. It contains all the fold's SSEs, including strand B and helix α_2 (see Figure 4b). In addition, the best alignment among four molecules consists solely of the CL family members. Their core consists of 104 residues with an RMSD of 1.2 Å. It contains the fold's SSEs, except for helix α_2 (which is missing in protein PDB:1f7s), the two additional CL helices and a small β-strand (see Figure 4c). For three molecules, there are two good alignments. The first alignment is between three out of the four CL structures. The outlier protein is PDB:1f7s, which lacks the C-terminal α-helix (α_2). The core of this alignment consists of 120 residues with an RMSD of 1.3 Å. It is similar to the core of all four CL structures, except that it contains also helix α_2 (see Figure 4d). The second good alignment of three molecules is between the three X-ray solved CL structures (PDB: 1f7s, 1cfyB and 1cnu) where the outlier is an NMR structure (PDB: 1ak6). Additionally, the three structurally similar proteins are classified as cofilin domains, while PDB:1ak6 is classified as destrin based on sequence similarity. The core of this alignment consists of 114 residues with an RMSD of 0.9 Å. It is similar to the core of all four CL structures.

This example demonstrates an application of MASS for the exploration of protein ensembles that are structurally homologous at different levels (e.g. family or fold). Multiple structural alignments of such ensembles are capable of addressing questions regarding the structural profile of a family and of a fold, and the structural characteristics that distinguish between different families within the same fold.

• **DNA-Binding Ensemble.** We find this ensemble interesting since the common denominator of the participating molecules is function and not fold (in contrast to the CL-GL ensemble). In such a case, one knows in advance that the ensemble may be structurally diverse, that is, it may contain different protein folds and thus poses a classification challenge.

The ensemble consists of 18 DNA-binding proteins, which can be classified into five structural groups (see Table 1). The proteins in each group belong to different domains of the same SCOP family or to different families of the same superfamily. The running time of MASS on this ensemble was 15 seconds. All five groups were detected as subset alignments (see Table 2 and Figure 6). The alignment of the classic zinc finger family captures a β-hairpin and an α-helix, together with the zinc atoms of the DNA-protein complexes. The alignment of the nucleosome core histones shows that they achieve a contact with DNA via their assembly. Their conserved structural core consists of three α-helices. The alignment of the phage repressor family shows the conservation of the helix-turn-helix DNA binding

site scaffold. The alignment of members from the 'restriction endonuclease like' superfamily has a core of a β-sheet and two α-helices. Here, the members are more remotely related and thus the structural core does not contain the DNA binding site. Finally, the alignment of the winged helix superfamily members has a structurally conserved core that contains a central two-stranded β-sheet and three α-helices. In this case the binding site is included in the alignment. Note that PDB:1fokA has two different domains that are differently classified in the SCOP database into the 'Restriction endonuclease-like' and the 'Winged helix DNA-binding domain' superfamilies. MASS detected the structural similarity within both input subsets.

The automatic detection, without any *a priori* knowledge of subset alignments of the different DNA binding molecules suggests that MASS is a powerful tool for structural classification of protein ensembles.

2.2 Detection of Non-Topological Motifs

The following example shows that MASS is capable of finding non-topological structural alignments, i.e. alignments in which the spatial configuration of the corresponding SSEs is conserved while their order and direction along the polypeptide chains are not conserved. Such alignments demonstrate that even when the sequences and topologies of proteins are totally different, their 3D structures may be surprisingly similar. In addition, such alignments may aid in elucidating the role of secondary structure packing preferences in protein folding. Here we give only one example for non-topological alignment. Other examples, obtained by MASS, can be found in (Dror *et al.*, 2003).

• **TRAF-Immunoglobulin Ensemble.** The eight proteins of this ensemble belong to two different folds of the all-β class in the SCOP database (Murzin *et al.*, 1995): (i) Four of these (PDB: 1czyA, 1kzzA, 1lb4 and 1k2fA) belong to the 'TRAF (TNF Receptor Associated Factor) domain-like' fold. There is only one superfamily in this fold and it consists of two families, 'TRAF domain' and SIAH ('Seven In Absentia Homolog'). Proteins PDB:1czyA, 1kzzA and 1lb4 were taken from the three domains of the TRAF family, where PDB:1k2fA was taken from the only domain of the SIAH family; (ii) The other proteins (PDB: 1bmg, 1frtB, 1igtA and 1k8iA) belong to four different domains of the 'C1 set domains' family of the 'Immunoglobulin-like beta-sandwich' fold.

The running time of MASS on this ensemble was 21 seconds. Figure 7a presents their structural alignment. The core of the alignment consists of 31 residues with an RMSD of 1.6Å. It forms a sandwich of 6 β-strands. Figures 7b and 7c show that the alignment is non-sequential and that the structurally conserved core appears in the various proteins via different topologies.

MASS also detected subset alignments. As expected, the highest scoring ones between four proteins are: (i) an alignment between all proteins of the 'TRAF domain-like' fold. The common core consists of 82 residues with an RMSD of 1.5Å. It forms a sandwich of eight β-strands (see Figure 8a); (ii) an alignment between all proteins of the 'Immunoglobulin-like beta-sandwich' fold. The core consists of 76 residues with an RMSD of 1.1Å, and it forms a sandwich of seven β-strands (see Figure 8b). Interestingly, these two subset alignments

are sequential, although in the alignment between all the eight proteins, the four members of each fold are aligned in a non-sequential manner. Specifically, proteins PDB:1k2fA and PDB:1k8iA are non-sequentially aligned with respect to the other three members of their fold (see Figure 7b). This demonstrates that an alignment, which is optimal for the whole set, is not always optimal for every subset.

The example demonstrates the ability of MASS to detect structural similarity among proteins that belong to different folds. Such structural similarity can not be detected by sequence alignment methods and not even by structural alignment methods, which are sequence-order dependent (e.g. methods that are based on dynamic programming).

2.3 Detection of Several Different Common Substructures

This section shows the ability of MASS to detect more than one common substructure (domain or motif) for a given set of molecules.

• **Detection of Two Common Domains.** We have used MASS to align five protein structures that have two common domains: 'p53-like transcription factors' and 'E set domains' (PDB codes: 1a02N, 1iknA, 1nfiA, 1imhA and 1a3qA). The running time was 19 seconds. MASS detected two different common substructures, one for each domain. The first common substructure is part of the 'p53-like transcription factors' domain. It consists of 114 residues with an RMSD of 1.4 Å and it forms a sandwich of nine β-strands (see Figure 9a). The second common substructure is part of the 'E set domains' domain. It consists of 87 residues with an RMSD of 1.2 Å and it forms a sandwich of seven β-strands (see Figure 9b). The two common substructures may indicate a possible hinge motion between the two domains, i.e. there is no 3D rigid transformation that simultaneously aligns the two domains. In future work we intend to extend MASS to handle hinge motions.

• **Detection of Two Common Motifs.** When we applied MASS to the DNA-Binding ensemble (see section 2.1), we obtained two good subset alignments for the three winged-helix proteins (PDB: 1fokA, 1ddnA and 1cgpA). The first alignment is the one that is described in section 2.1. Its core consists of a bundle of three helices and a small β-sheet (46 residues with an RMSD of 1.7 Å). Although the core of the second alignment also forms a motif of a 3-helix bundle and a small β-sheet (45 residues with an RMSD of 1.6 Å), the two alignments are different. Figures 10a and 10b show the two alignments respectively. As one can see, the transformation that superimposes PDB:1ddnA onto PDB:1cgpA (the pivot structure) is similar in the two alignments, but the transformation that superimposes PDB:1fokA onto PDB:1cgpA is completely different. This indicates that the winged-helix motif appears twice in PDB:1fokA. Figure 10c shows that two detected motifs of PDB:1fokA are involved in DNA binding.

The above examples demonstrate that the largest common substructure is not the only biologically interesting solution and emphasize the need to examine a list of high-scoring solutions, rather than only the highest one.

2.4 Large-Scale Structural Alignments

Here we demonstrate MASS's capability of aligning tens of protein structures in practical running times on a standard PC. For this purpose, we have applied MASS to the following four SCOP ensembles (Murzin *et al.*, 1995): (i) TIM-barrels - all of the 62 structures, which belong to the Xylose isomerase family of the TIM beta/alpha-barrel fold (the family consists of only one domain); (ii) Microbial ribonucleases - all 63 structures belonging to the RNase T1 domain of the Microbial ribonucleases family; (iii) Subtilisin - all 60 structures belonging to the Subtilisin domain of the Subtilases family; and (iv) unrelated proteins - a compiled set of 60 unrelated protein structures. Each structure was taken from a different fold of the four major SCOP classes: all-α, all-β, α+β and $\alpha\backslash\beta$.

Table 3 summarizes the performance of MASS on the four ensembles as a function of: (i) the number of molecules; (ii) the average molecular size; (iii) the average number of SSEs in a molecule; and (iv) the structural similarity among the molecules. All four parameters increase the running time as they grow. Both our complexity analysis and results demonstrate such a behavior. For instance, although the Microbial ribonucleases and the Tim-barrel ensembles consist of almost the same number of proteins taken from the same SCOP domain (63 and 62 respectively), the running time of MASS on the Microbial ribonucleases ensemble (28 sec) is much shorter than on the Tim-barrel ensemble (47min:59sec). This difference in the running times is mainly due to the difference in the average molecular size and the average number of SSEs (103 and 3 vs. 391 and 14 respectively). Another factor that has influenced the running time is the difference in the number of self recurring motifs. The TIM-barrel proteins have more self recurring motifs due to their symmetric structures. As a result, more bases were stored in a bucket's column and the runtime was increased. Comparing the performance of MASS on the Subtilisin ensemble and on the compiled set of unrelated proteins shows how structural variance among the input proteins influences the running time: The more structurally variable is the ensemble, the shorter the running time is. Both ensembles consist of 60 molecules, their average number of SSEs is 14 and their average molecule size is almost the same (273 and 297), even though the running time of MASS on the compiled set of unrelated proteins (9min:42sec) is shorter than on the Subtilisin ensemble (23min:10sec). We attribute this difference in the running times mainly to the difference in the structural variance within each ensemble: The Subtilisin ensemble consists of structurally homogeneous proteins (i.e. proteins from the same SCOP domain) where the other ensemble consists of structurally unrelated proteins (i.e. each protein belongs to a different SCOP fold).

3 Application of MASS for Docking Improvements

The problem of predicting the correct binding mode of protein-protein interaction is extremely difficult. A major problem is that of 'false positives'. In the state-of-the-art docking algorithms often a correct solution (within 5Å RMSD from the native complex) is detected among the best few hundreds, alas it is ranked too low to be analyzed by a subsequent visual inspection (Halperin *et al.*, 2002). This problem is especially acute for large protein molecules, where there are alternative binding interfaces with better complementarity.

Therefore, an *a priori* knowledge of the binding site is likely to critically aid in detecting the correct docking. Sometimes the binding site is known in advance due to direct biochemical data. In the absence of such knowledge, one may need to utilize alternative means. Here we show how an efficient multiple structure comparison routine, such as MASS, can be helpful in guiding protein-protein docking.

The serine proteinases have been a standard benchmark for evaluating multiple structural alignment methods (Yang & Honig, 2000*b*; Russell & Barton, 1992; Sali & Blundell, 1990). In particular, the ten serine proteinases listed in Table 4 are known to be difficult to align using sequence information alone (Russell & Barton, 1992). Figure 11a shows the structural alignment of all ten proteins as obtained by MASS (runtime 39 seconds). A structural core of 123 residues is detected with an RMSD of 1.5Å. It contains the two six-stranded antiparallel β-barrels that form the fold and the three residues of the *catalytic triad* (HIS-57, ASP-102, SER-195). MASS further detected three conserved loops: residues 55-59 (contains a small $3-10$ helix), 128-130 and 189-197. Two of these contain residues that belong to the catalytic triad (His-57, Ser-195).

Secondary structures serve as the scaffold of proteins and thus are usually conserved for stability purposes. In contrast, conservation of connecting loops may indicate a potential functional site. A docking of kallikrein A (PDB:2pkaAB) and a bovine pancreatic trypsin inhibitor (PDB:6pti) was performed using PatchDock (Duhovny *et al.*, 2002). We applied the docking procedure twice: (i) without any assumption on the binding site; (ii) a guided docking, defining the structurally conserved loops detected by MASS as the region that contains the binding site. Strikingly, the rank of the correct docking solution was improved from 49 to 1 (see Figure 11b).

4 Conclusions

Here we have described a novel method, named MASS, for aligning multiple protein structures and detecting their common structural motifs. MASS simultaneously compares the input proteins, both at the secondary structure and the C_α atomic levels. The usage of SSEs at the first stage aids in filtering out noisy solutions and in making the method highly efficient and robust.

The results have demonstrated the performance of MASS on some challenging cases of multiple structural alignment. We have shown that: (i) MASS is capable of aligning tens of protein structures in practical running time; (ii) As MASS disregards the sequence order of SSEs, it is able to detect non-topological structural motifs; and (iii) MASS can successfully detect biologically meaningful substructures common to non-predefined subsets of the input ensemble. It automatically classifies the given ensemble to its constituent structural and functional subsets. For example, it distinguished between different families of DNA binding proteins. We have further shown a new application of multiple structure alignment: exploiting the detected structurally conserved motifs for considerably improving the results of a docking procedure.

These features of MASS suggest that it is a useful tool for homology modeling, protein classification and structure-function studies. We further suggest the SSE-only mode of MASS

as a potential future application. Compared to the full (SSE and atomic) mode, the SSE-only mode is far more efficient with lower running times. It may be useful for two types of cases: (i) Large scale ensembles. Currently, MASS exhibits practical running times on ensembles on the order of tens of proteins. Using SSE-only mode is likely to enable the running of MASS on larger ensembles. (ii) Ensembles that contain proteins for which only SSE information exists. Examples include theoretical models obtained by structure prediction methods, or suggested SSE arrangements inferred from cryo-electron microscopy (Chiu *et al.*, 2002).

Acknowledgments. We thank Dina Schneidman-Duhovny for contributing the docking result of the serine proteinase. This research has been supported in part by the "Center of Excellence in Geometric Computing and its Applications" funded by the Israel Science Foundation (administered by the *Israel Academy of Sciences*). The research of H.J. Wolfson and O. Dror is partially supported by the Hermann Minkowski-Minerva Center for Geometry at Tel Aviv University. The research of R. Nussinov has been funded in whole or in part with Federal funds from the National Cancer Institute, National Institutes of Health, under contract number NO1-CO-12400. The content of this publication does not necessarily reflect the view or policies of the Department of Health and Human Services, nor does mention of trade names, commercial products, or organization imply endorsement by the U.S. Government.

References

Akutsu T, Halldorsson MM. 2000. On the approximation of largest common subtrees and largest common point sets. *Theor. Comput. Sci.* **233**: 33–50.

Akutsu T, Sim KL. 1999. Protein threading based on multiple protein structure alignment. *Genome Informatics* **10**: 23–29.

Alesker V, Nussinov R, Wolfson H. 1996. Detection of non-topological motifs in protein structures. *Protein Eng.* **9**: 1103–1119.

Alexandrov N, Fischer D. 1996. Analysis of topological and nontopological structural similarities in the PDB: new examples with old structures. *Proteins* **25**: 354–365.

Andersen C, Palmer A, Brunak S, Rost B. 2002. Continuum secondary structure captures protein flexibility. *Structure* **10**: 175–185.

Bachar O, Fischer D, Nussinov R, Wolfson H. 1993. A computer vision based technique for 3-D sequence independent structural comparison. *Protein Eng.* **6**: 279–288.

Benyamini H, Gunasekaran K, Wolfson H, Nussinov R. 2003. Conservation and amyloid formation: a study of the gelsolin-like family. *Proteins* **51**: 266–281.

Berman H, Westbrook J, Feng Z, Gilliland G, Bhat T, Weissig H, Shindyalov I, Bourne P. 2000. The protein data bank. *Nucleic Acids Res.* **28**: 235–242.

Branden C, Tooze J. 1999. *Introduction to Protein Structure, Second Edition*. New York: Garland Publishing, Inc.

Brown NP, Orengo CA, Taylor WR. 1996. A protein structure comparison methodology. *Comput. Chem.* **20**: 359–380.

Chiu W, Baker M, Jiang W, Zhou Z. 2002. Deriving folds of macromolecular complexes through electron cryomicroscopy and bioinformatics approaches. *Curr. Opin. Struct. Biol.* **12**: 263–269.

Ding D, Qian J, Feng Z. 1994. A differential geometric treatment of protein structure comparison. *Bull. Math. Biol.* **56**: 923–943.

Dror O, Benyamini H, Nussinov R, Wolfson H. 2003. MASS: multiple structural alignment by secondary structures. *Bioinformatics* **19 Suppl. 1**: i95–i104.

Duhovny D, Nussinov R, Wolfson H. 2002. Efficient unbound docking of rigid molecules. In *Workshop on Algorithms in Bioinformatics*, (Guigo R, Gusfield D, eds), pp. 185–200, Springer Verlag, Rome, Italy. Lecture Notes in Computer Science 2452.

Eidhammer I, Jonassen I, Taylor W. 2001. Structure comparison and structure patterns. *J. Comp. Biol.* **7**: 685–716.

Escalier V, Pothier J, Soldano H, Viari A. 1988. Pairwise and multiple identification of three-dimensional common substructures in proteins. *J. Comp. Biol.* **5**: 41–56.

Flores T, Moss D, Thornton J. 1994. An algorithm for automatically generating protein topology cartoons. *Protein Eng.* **7**: 31–37.

Gerstein M, Levitt M. 1996. Using iterative dynamic programming to obtain accurate pairwise and multiple alignments of protein structures. In *Proceedings of the Fourth International Conference on Intelligent Systems for Molecular Biology*, (States DJ, Agarwal P, Gaasterland T, Hunter L, Smith R, eds), pp. 59–67, The AAAI press, Menlo Park, California.

Grindley H, Artymiuk P, Rice D, Willett P. 1993. Identification of tertiary structure resemblance in proteins using a maximal common subgraph isomorphism algorithm. *J. Mol. Biol.* **229**: 707–721.

Guda C, Scheeff E, Bourne P, Shindyalov I. 2001. A new algorithm for the alignment of multiple protein structures using monte carlo optimization. In *Proceedings of the Pacific Symposium on Biocomputing*, (Altman RB, Dunker AK, Hunker L, Lauderdale K, Klein TE, eds), pp. 275–286, World Scientific, Singapore.

Gusfield D. 1993. Efficient methods for multiple sequence alignment with guaranteed error bounds. *Bull. Math. Biol.* **55**: 141–154.

Halperin I, Ma B, Wolfson H, Nussinov R. 2002. Principles of docking: an overview of search algorithms and a guide to scoring functions. *Proteins* **47**: 409–443.

Hatanaka H, Ogura K, Moriyama M, Ichikawa S, Yahara I, Inagaki F. 1996. Tertiary structure of destrin and structural similarity between two actin-regulating protein families. *Cell* **85**: 1047–1055.

Holm L, Sander C. 1995. 3-D lookup: fast protein structure database searches at 90% reliability. In *Proceedings of the Third International Conference on Intelligent Systems for Molecular Biology*, (Rawlings CJ, Clark DA, Altman RB, Hunter L, Lengauer T, Wodak SJ, eds), pp. 179–187, The AAAI press, Menlo Park, California.

Kabsch W. 1978. A discussion of the solution for the best rotation to relate two sets of vectors. *Acta. Cryst.* **A 34**: 827–828.

Kabsch W, Sander C. 1983. Dictionary of protein secondary structure: pattern recognition of hydrogen-bonded and geometrical features. *Biopolymers* **22**: 2577–2637.

Kaindl K, Steipe B. 1997. Metric properties of the root-mean-square deviation of vector sets. *Acta. Cryst.* **A53**: 809.

Koch I, Lengauer T, Wanke E. 1996. An algorithm for finding maximal common subtopologies in a set of proteins. *J. Comp. Biol.* **3**: 289–306.

Lamdan Y, Wolfson H. 1988. Geometric hashing: a general and efficient model-based recognition scheme. In *Proceedings of the IEEE International Conference on Computer Vision* pp. 238–249, IEEE Computer Society Press, Tampa, Florida, USA.

Lehninger AL, Nelson DL, Cox MM. 1993. *Principles of Biochemistry, Second Edition*. New York: Worth Publishers.

Leibowitz N, Fligelman Z, Nussinov R, Wolfson H. 2001*a*. Automated multiple structure alignment and detection of a common motif. *Proteins* **43**: 235–245.

Leibowitz N, Nussinov R, Wolfson H. 2001*b*. MUSTA - a general efficient, automated method for multiple structure alignment and detection of common motifs: application to proteins. *J. Comp. Biol.* **8**: 93–121.

Lemmen C, Lengauer T. 2000. Computational methods for the structural alignment of molecules. *J. Comput. Aided Mol. Des.* **14**: 215–232.

Lu G. 2000. TOP: a new method for protein structure comparisons and similarity searches. *J. Appl. Crystal.* **33**: 176–183.

May A, Johnson M. 1995. Improved genetic algorithm-based protein structure comparisons: pairwise and multiple superpositions. *Protein Eng.* **8**: 873–882.

Mitchel E, Artymiuk P, Rice D, Willet P. 1989. Use of techniques derived from graph theory to compare secondary structure motifs in proteins. *J. Mol. Biol.* **212**: 151–166.

Murzin A, Brenner S, Hubbard T, Chothia C. 1995. SCOP: a structural classification of proteins database for the investigation of sequences and structures. *J. Mol. Biol.* **247**: 536–540. `http://scop.berkeley.edu/`.

Needleman S, Wunsch C. 1970. A general method applicable to the search for similarities in amino acid sequence of two proteins. *J. Mol. Biol.* **48**: 443–453.

Nussinov R, Wolfson H. 1991. Efficient detection of three-dimensional strcutural motifs in biological macromolecules by computer vision techniques. *Proc. Natl. Acad. Sci. USA* **88**: 10495–10499. Biophysics.

Russell R, Barton G. 1992. Multiple protein sequence alignment from tertiary structure comparison: assignment of global and residue confidence levels. *Proteins* **14**: 309–323.

Sali A, Blundell T. 1990. Definition of general topological equivalence in protein structures. a procedure involving comparison of properties and relationships through simulated annealing and dynamic programming. *J. Mol. Biol.* **212**: 403–428.

Sayle R, Milner White E. 1995. RasMol: biomolecular graphics for all. *Trends Biochem. Sci.* **20**: 374–376.

Shatsky M, Nussinov R, Wolfson H. 2002. MultiProt - a multiple protein structural alignment algorithm. In *Workshop on Algorithms in Bioinformatics*, (Guigo R, Gusfield D, eds), pp. 235–250, Springer Verlag, Rome, Italy. Lecture Notes in Computer Science 2452.

Taylor WR, Flores T, Orengo C. 1994. Multiple protein structure alignment. *Prot. Sci.* **3**: 1858–1870.

Yang AS, Honig B. 2000*a*. An integrated approach to the analysis and modeling of protein sequences and structures. I. Protein structural alignment and a quantitative measure for protein structural distance. *J. Mol. Biol.* **301**: 665–678.

Yang AS, Honig B. 2000*b*. An integrated approach to the analysis and modeling of protein sequences and structures. III. A comparative study of sequence conservation in protein structural families using multiple structural alignments. *J. Mol. Biol.* **301**: 691–711.

Tables

Table 1: **DNA-Binding Ensemble.** Classification of the DNA-binding proteins into five different structural subgroups according to the SCOP database (Murzin *et al.*, 1995).

SCOP Classification	PDB Codes
Classic zinc finger (C2H2) family	1a1i, 1bhi, 1rmd, 1tf3, 1ubd, 1yuj, 5znf
Nucleosome core histones family	1hq3C, 1hq3D, 1eqzB
Phage repressors family	1perL, 2cro, 1adr
Restriction endonuclease-like superfamily	1cw0A, 1fokA, 3bamA
Winged helix DNA-binding domain superfamily	1fokA, 1ddnA, 1cgpA

Table 2: **DNA-Binding Ensemble.** The structural core detected by MASS for each of the five different structural subgroups listed in Table 1.

SCOP Classification	Core Size	RMSD	Core Description
Classic zinc finger (C2H2) family	20	1.2	β-hairpin followed by an α-helix
Nucleosome core histones family	65	1.4	a bundle of 3 helices
Phage repressors family	60	0.9	5 helices
Restriction endonuclease-like superfamily	55	1.9	β-sheet of 5 strands and 2 helices
Winged helix DNA-binding domain superfamily	46	1.7	a bundle of 3 helices and a small β-sheet (wing)

Table 3: **Run times of MASS on large-scale protein ensembles.** The performance of MASS as a function of: (i) the number of molecules; (ii) the average molecular size; (iii) the average number of SSEs in a molecule; and (iv) the structural similarity among the molecules. All four parameters increase the running time as they grow.

Ensemble Name	No. of Mol.	Avg. Mol. Size	Avg. No. of SSEs	SCOP classification	Run Time (h:mm:ss)
TIM-barrels	62	391	14	same domain	00:47:59
Microbial ribonucleases	63	103	3	same domain	00:00:28
Subtilisin	60	273	14	same domain	00:23:10
unrelated proteins	60	297	14	unrelated	00:09:42

Table 4: **Data Set.** The first four letters of a protein name are the PDB code, followed by chain id and the residue numbers for the first and the last residue.

Ensemble Name	PDB Codes
CL-GL	1f7s, 1ak6 ,1cfyB, 1cnu, 1d0nA:27-152, 1d0nA:153-262, 1d0nA:263-383, 1d0nA:384-532, 1d0nA:533-628, 1d0nA:629-755, 1svy, 2vik
DNA-Binding	1a1i, 1bhi, 1rmd, 1tf3, 1ubd, 1yuj, 5znf, 1hq3C, 1hq3D, 1eqzB, 1perL, 2cro, 1adr, 1cw0A, 1fokA, 3bamA, 1ddnA, 1cgpA
TRAF-Immunoglobulin	1czyA, 1kzzA, 1lb4, 1k2fA, 1bmg, 1frtB, 1igtA, 1k8iA
Two-Domains	1a02N, 1iknA, 1nfiA, 1imhA, 1a3qA
Serine Proteinases	1sgt, 1ton, 2alp, 2pkaAB, 2sga, 3est, 3rp2A, 3sgbE, 4chaA, 2ptn
TIM-barrels	6xia, 1dxiA, 2gyiA, 1xyaA, 1xylA, 1xymA, 1xybA, 1xycA, 4xis, 1xis, 1gw9A, 3xis, 1xib, 1xic, 1xif, 2xis, 1xii, 1xij, 1xih, 1xid, 1xig, 1xie, 9xia, 8xia, 1qt1A, 1clkA, 4xiaA, 1xlmA, 1dieA, 1xlaA, 1xlcA, 1xldA, 1xlfA, 1xlhA, 1xliA, 5xiaA, 1didA, 1xlgA, 1xljA, 1xlbA, 1xllA, 1xlkA, 1xleA, 1ximA, 3ximA, 5xinA, 4ximA, 3xinA, 2xinA, 2ximA, 7ximA, 9ximA, 8ximA, 1xinA, 6ximA, 5ximA, 1bhwA, 1a0cA, 1a0dA, 1a0eA, 1bxcA, 1bxbA
Microbial ribonucleases	1i0vA, 9rnt, 1loyA, 1lovA, 1rga, 4gsp, 1i0xA, 8rnt, 2rnt, 3rnt, 1i3iA, 4bir, 1rgk, 2aae, 5bu4A, 1hyfA, 2gsp, 6rnt, 1fzuA, 1rn4, 5gsp, 1i2gA, 3gsp, 1i2eA, 2hohA, 4bu4A, 1g02A, 3bu4A, 3hohA, 1birA, 1bviA, 1rhlA, 1det, 1bu4, 1i2fA, 5hohA, 1rls, 1rgl, 7gspA, 1fysA, 5birA, 2aadA, 1lra, 1rgcA, 7rnt, 2bu4A, 1rnt, 1lowA, 1gsp, 1b2mA, 4hohA, 1rn1A, 6gsp, 4rnt, 1trqA, 1i3fA, 1ch0A, 3bir, 2birA, 1trpA, 5rnt, 1ygw, 1hz1A
Subtilisin	1cseE, 2secE, 1selA, 1sbc, 1scjA, 1bh6A, 1avt, 1sca, 1scnE, 1vsb, 1c3lA, 1scd, 1be8, 1be6, 1bfu, 1bfk, 3vsb, 1av7, 1af4, 1scb, 1svn, 1gci, 1st3, 1jea, 1c9nA, 1c9mA, 1c9jA, 1lw6E, 1sup, 1a2q, 1s01, 1aqn, 1sub, 2st1, 1au9, 1ak9, 1yjb, 1sbh, 1sue, 1suc, 2sicE, 1s02, 1gnvA, 3sicE, 1yjc, 1sud, 1yja, 1gnsA, 1st2, 2sniE, 1duiA, 1spbS, 1suaA, 1sbi, 1sbnE, 1ubnA, 5sicE, 1sibE, 1sbt, 2sbt

Continued on next page

Table 4 – continued from previous page

Ensemble Name	PDB Codes
unrelated proteins	1ah7, 1aorA:211-605, 1bkdS, 1bqv, 1csh, 1dnpA:201-469, 1dz4A, 1ewqA:267-541, 1f0jA, 1f5nA:284-583, 1g9lA, 1hbnA:270-549, 1i7wA, 1jswA, 1lla110-379, 1air, 1aol, 1arb, 1at0, 1gof151-537, 1hcb, 1ijaA, 1k8hA, 1knb, 1l7kA, 1lxa, 1nls, 1ospO, 1p35A, 1qexA, 1ad3A, 1cjyA:142-721, 1cm5A, 1dhs, 1ds9A, 1eu1A:4-625, 1fehA:210-574, 1gr8A, 1jetA, 1jixA, 1k30A, 1qpg, 1tml, 1ttqB, 1xaa, 1ag2, 1c8zA, 1cby, 1cfe, 1cnsA, 1d8iA, 1dy5A, 1ji8A, 1kyfA:825-938, 1kypA, 1mut, 1nox, 1qndA, 1qqqA, 1sryA:111-421

Figure Legends

Figure 1: **The flow of the MASS algorithm.** MASS is based on a two-level alignment, using both secondary structure and atomic representation. In the first stage, the protein structures are represented by their SSEs and initial local alignments are obtained based on this coarse representation. In the second stage, we use the C_α atomic coordinates of the protein structures to refine and extend the initial alignments in order to obtain global atomic superpositions. However, note that when atomic information is not available, there is an option in MASS to obtain alignments based only on secondary structures. In this mode, the local base alignment, clustering and filtering steps are performed at the SSE level.

Figure 2: **SSE representation. (a)** Representing a helix as a 3D directed line segment. **(b)** The line segment that represents an SSE is defined as follows: (i) its line is the *least square line* of all the C_α atoms of the SSE, i.e. the line that minimizes $\sum_{C_\alpha \in SSE} d_i^2$; (ii) its length is determined by the projection of the two terminal C_α atoms of the SSE; and (iii) its direction is from the N-terminus to the C-terminus.

Figure 3: **Base fingerprint and Base Bucket. (a)** The fingerprint of a base is defined as a 5D vector composed of the types of the two SSEs, the angle (α) between their axial vectors, the midpoint-to-midpoint distance between their axes and their line distance. **(b)** A base bucket stores almost-congruent bases. The bases are stored in columns according to the protein they belong to. The paths shown in red, green and magenta are examples for possible multiple base alignments.

Figure 4: **CL-GL ensemble.** The figure shows four different subset alignments. The backbone of the proteins is displayed in RasMol strands representation (Sayle & Milner-White, 1995) and is colored gray. The structurally conserved core detected by MASS is colored by secondary structure (helices are colored magenta, strands are colored yellow, turns are colored blue, and all other residues are colored light gray). **(a)** The structural alignment of all twelve proteins of the ensemble. **(b)** A subset alignment between only the eight GL proteins. **(c)** A subset alignment between only the four CL structures. **(d)** A subset alignment between only three out of the four CL structures. The outlier is PDB:1f7s, which lacks the C-terminal α-helix.

Figure 5: **CL-GL ensemble.** The graph presents the maximal core size for every number of aligned molecules, taken from the CL-GL ensemble.

Figure 6: **DNA-Binding ensemble.** Subset alignments that captured the five structural subgroups of the ensemble: classic zinc finger, nucleosome core histones, phage repressors, restriction endonuclease and winged helix (see Table 1). The backbone of the proteins is displayed in RasMol strands representation (Sayle & Milner-White, 1995) and colored in gray. The conserved regions of the proteins are colored by secondary structure. The DNA is shown in spacefill representation and colored in light yellow. **(a)** The alignment of all seven structures of the 'Classic zinc finger (C2H2)' family. Four of the structures are DNA-complexes. Only the DNA from PDB:1yuj is shown. The Zinc atoms of all four DNA-complexes are displayed by assigning a different color to each complex. As one can see, the

four Zinc atoms are strictly superimposed. **(b)** The alignment of all three structures of the 'Nucleosome core histones' family. The DNA is from PDB:1eqzB. **(c)** The alignment of all three structures of the 'Phage repressors' family. The displayed DNA is of PDB:1perL. **(d)** The alignment of all three structures of the 'Restriction endonuclease-like' superfamily. The displayed DNA is from PDB:1fokA. **(e)** The alignment of all three structures of the 'Winged helix DNA-binding domain' superfamily. The displayed DNA is from PDB:1cgpA.

Figure 7: **TRAF-Immunoglobulin ensemble. (a)** The structural alignment of all eight proteins of the ensemble. The backbone of the proteins is displayed in RasMol strands representation (Sayle & Milner-White, 1995) and is colored in gray. Their common core is displayed by assigning a different color to each of the six conserved β-strand. **(b)** The match between the conserved β-strands (E stands for a β-strand and it is followed by the strand number along the polypeptide chain). Note that a strand was not assigned to residues 3-7 of protein PDB:1igtA by the DSSP program (Kabsch & Sander, 1983). But, according to the PDB assignment, residues 4-7 form a strand. **(c)** The TOPS diagrams of the proteins (Flores *et al.*, 1994). Triangles represent strands and circles helices as assigned by the DSSP program (Kabsch & Sander, 1983). Corresponding strands are drawn in the same color. As one can see the alignment is non-topological and its core is a β-sandwich.

Figure 8: **TRAF-Immunoglobulin ensemble.** The figure shows that MASS has managed to distinguish between the 'TRAF domain-like' and the 'Immunoglobulin-like beta-sandwich' proteins. The backbone of the proteins is displayed in RasMol strands representation (Sayle & Milner-White, 1995) and colored in gray. The conserved regions of the proteins are colored by secondary structure (helices are colored magenta, strands are colored yellow, turns are colored blue, and all other residues are colored light gray). **(a)** A subset alignment between only the four proteins of the 'TRAF domain-like' fold. **(b)** A subset alignment between only the four proteins of the 'Immunoglobulin-like beta-sandwich' fold.

Figure 9: **Two-Domains ensemble.** The figure shows the two different structural conserved cores of the ensemble. The backbone of protein 1nfiA is shown in navy. The backbone of the other proteins is colored gray. The two structurally conserved cores detected by MASS are colored by secondary structure. **(a)** The first detected conserved core (part of the 'p53-like transcription factors' domain). **(b)** The second detected conserved core (part of the 'E set domains' domain).

Figure 10: **Winged Helix DNA-Binding Domain.** The figure shows the two different subset alignments that were obtained for the three winged helix DNA-binding proteins (PDB: 1cgpA, 1fokA, 1ddnA) when we applied MASS to the DNA-Binding ensemble. The backbone of the proteins is colored gray. The cores of the alignments are colored by secondary structure. The DNA of PDB:1cgpA, 1fokA and 1ddnA are colored in light yellow, light blue and light pink respectively. **(a)** The first detected subset alignment (also shown in Figure 6e). The DNAs of all the three complexes are well aligned. The core of the alignment is a winged-helix motif (three helices and a small β-sheet). **(b)** The second detected subset alignment. Only the DNAs of PDB:1cgpA and PDB:1ddnA are well aligned. The core of this alignment is also a winged-helix motif. **(c)** The figure shows that the two detected winged-helix motifs of PDB:1fokA are involved in DNA binding.

Figure 11: **Serine Proteases.** **(a)** The structural alignment of ten serine proteinases. PDB:2pkaAB is shown completely in light yellow. The core of the alignment is colored by secondary structure and the three conserved loops are colored in green. The catalytic triad is also conserved (the triad of PDB:2pkaAB is depicted as ball-and-sticks and colored dark blue). Two of the conserved loops (55-59 and 189-197) are located in the active site. **(b)** The unbound docking, as obtained by PatchDock (Duhovny *et al.*, 2002), between a 'serine protease kallikrein A' (PDB:2pka) and its bovine pancreatic trypsin inhibitor (PDB:6pti). The receptor PDB:2pka is depicted as in (a). The docked inhibitor, colored in red, is superimposed on the inhibitor of the crystal complex (PDB:2kaiI), colored blue.

Figures

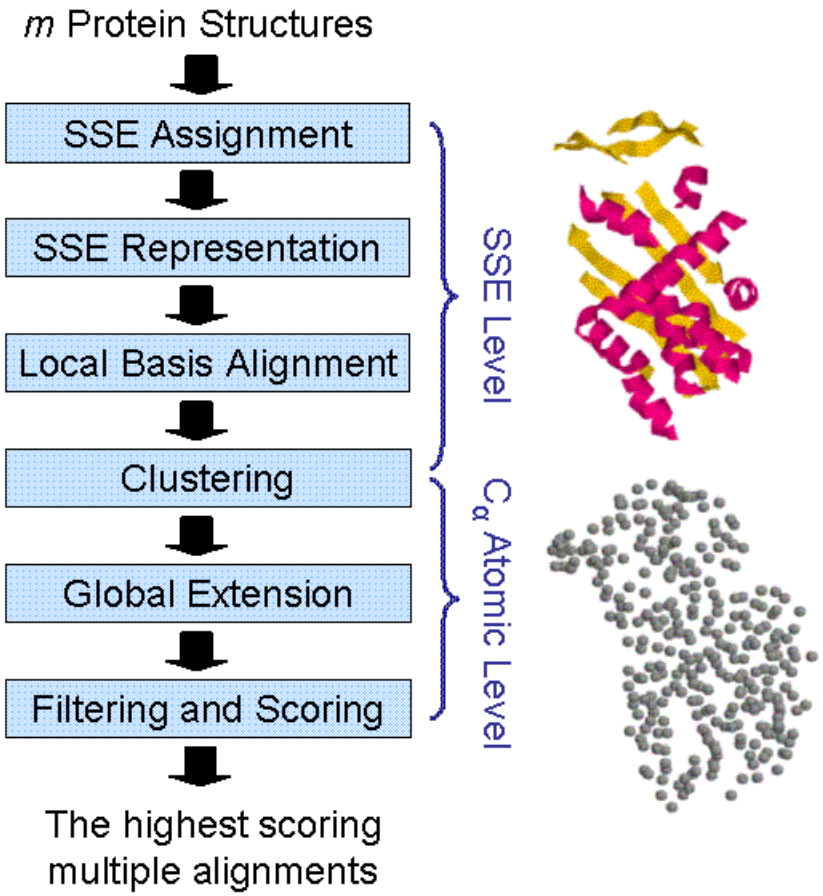

Figure 1.

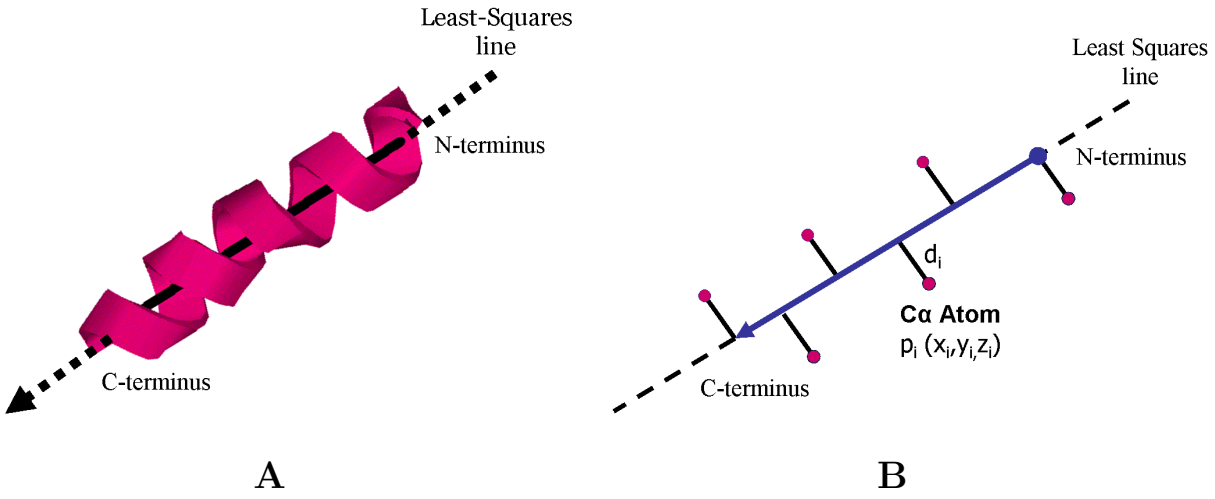
Least-Squares
line
N-terminus
C-terminus
A
Least Squares
line
N-terminus
d_i
Cα Atom
p_i (x_i,y_i,z_i)
C-terminus
B

Figure 2.

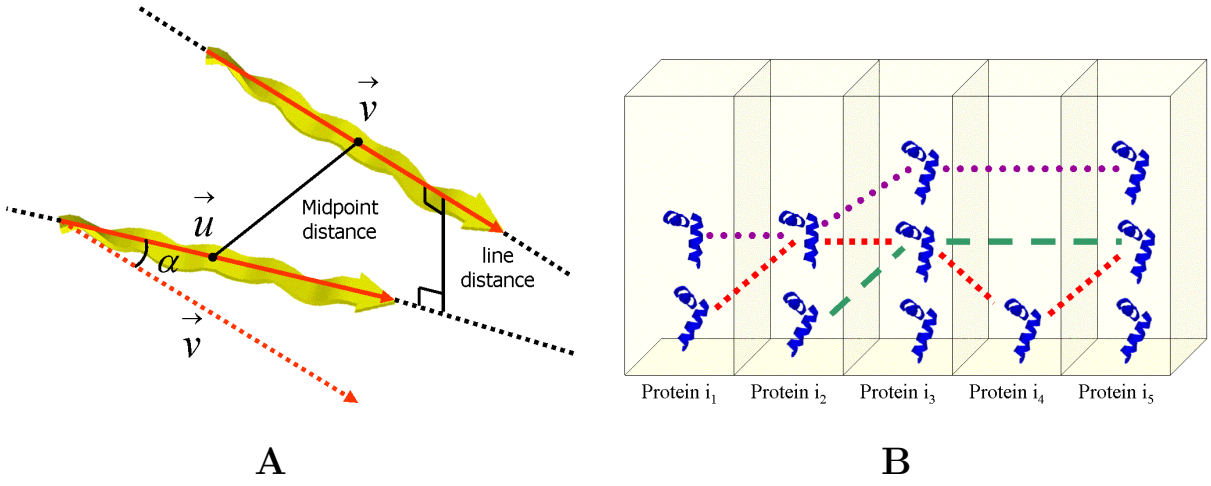
$\vec{v}$
$\vec{u}$
α
Midpoint distance
line distance
$\vec{v}$
Protein i_1
Protein i_2
Protein i_3
Protein i_4
Protein i_5
A
B

Figure 3.

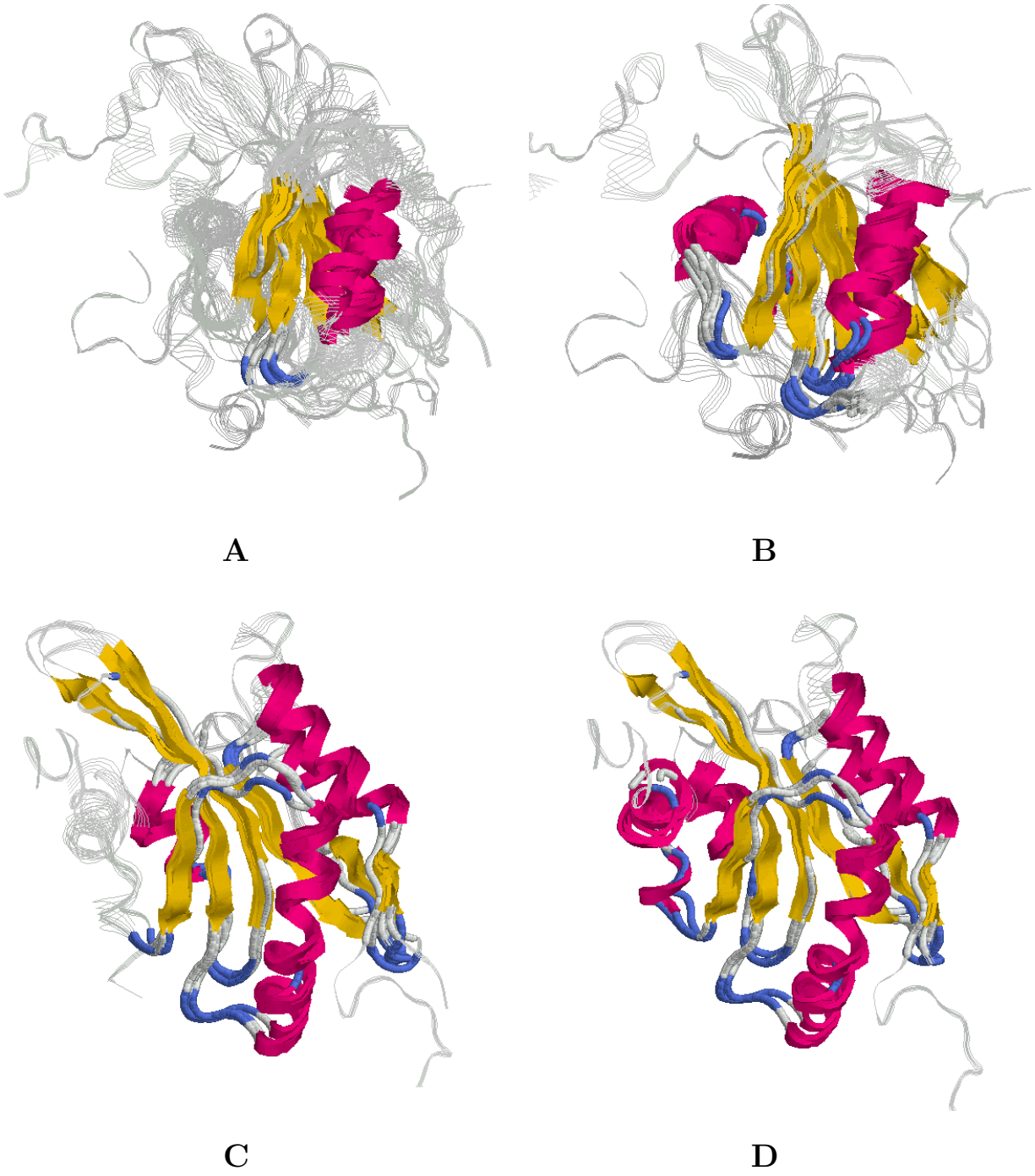

Figure 4.

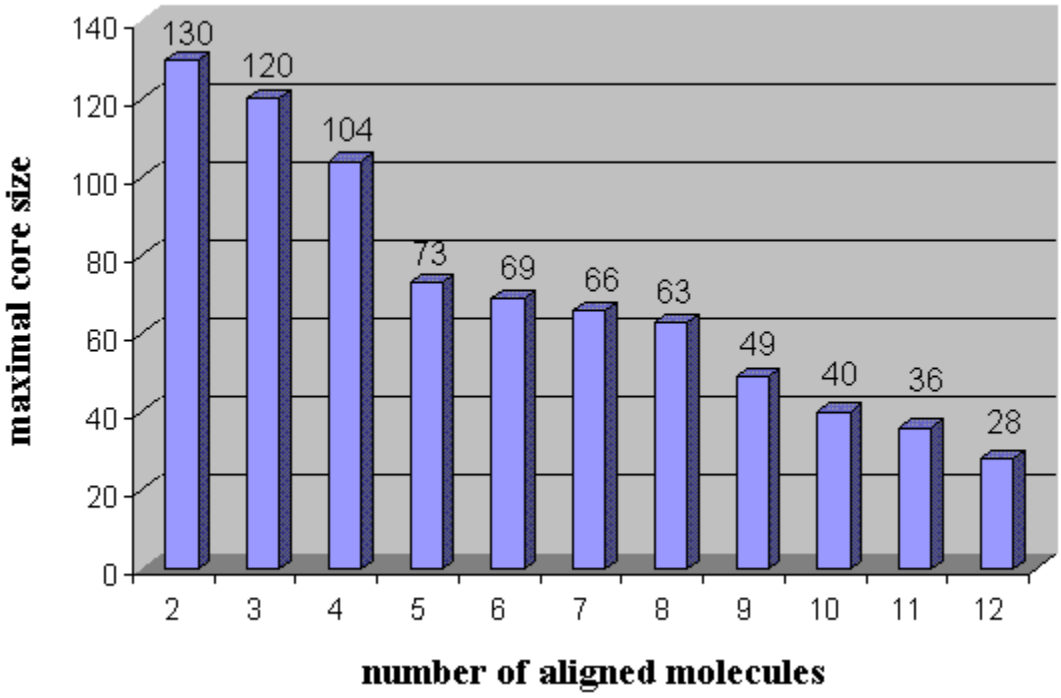
maximal core size
140
120
100
80
60
40
20
0
130
120
104
73
69
66
63
49
40
36
28
2
3
4
5
6
7
8
9
10
11
12
number of aligned molecules

Figure 5.

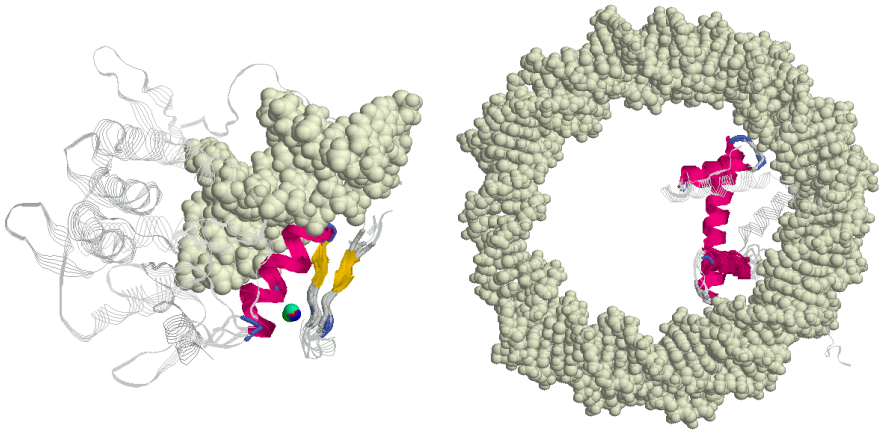

A **B**

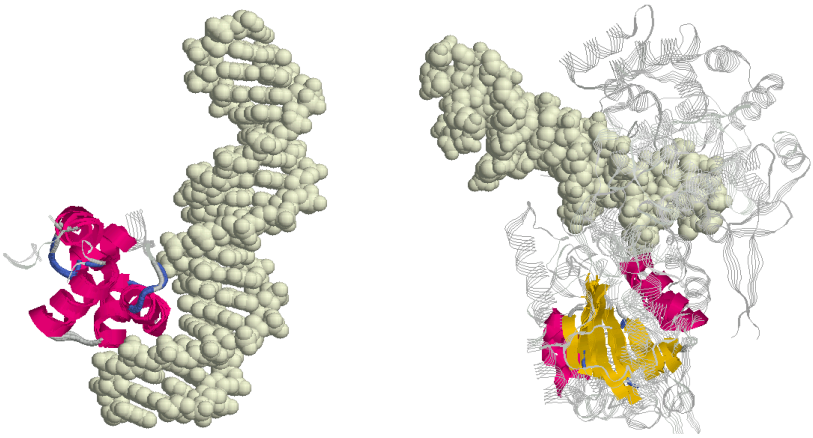

C **D**

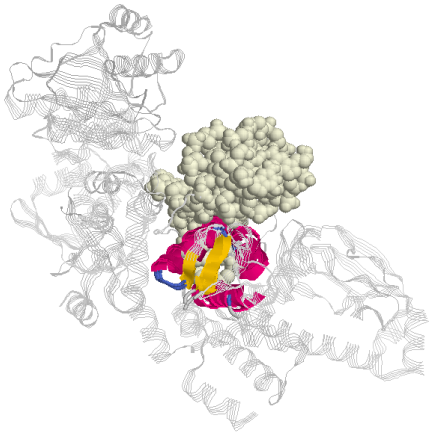

E

Figure 6.

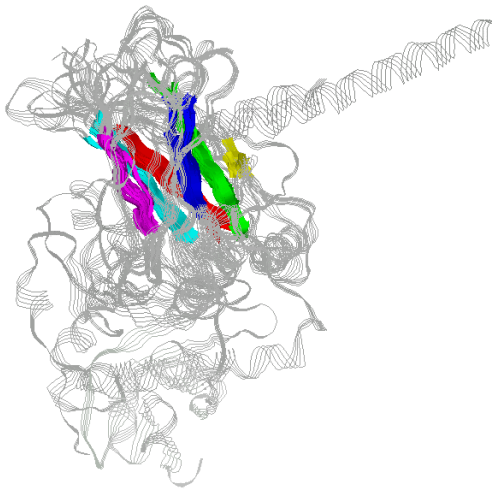

1czyA	1kzzA	1lb4A	1k2fA	1bmg	1frtB	1igtA	1k8iA
E0	E0	E0	E4	E6	E6	E6	E5
E1	E1	E1	E3	E3	E3	E3	E11
E3	E2	E3	E11	E2	E2	E2	E10
E4	E3	E4	E7	E7	E7	E7	E6
E5	E4	E5	E6	E0	E0	3-7	E8
E8	E6	E8	E5	E1	E1	E1	E9

A **B**

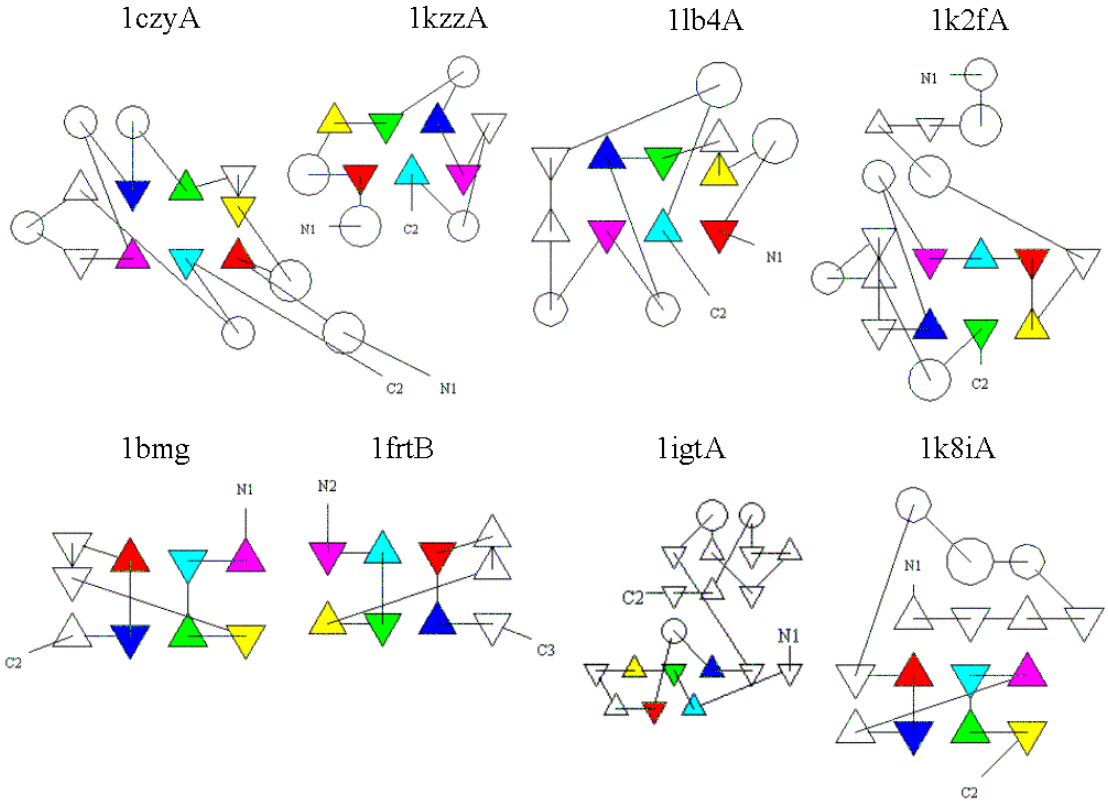

C

Figure 7.

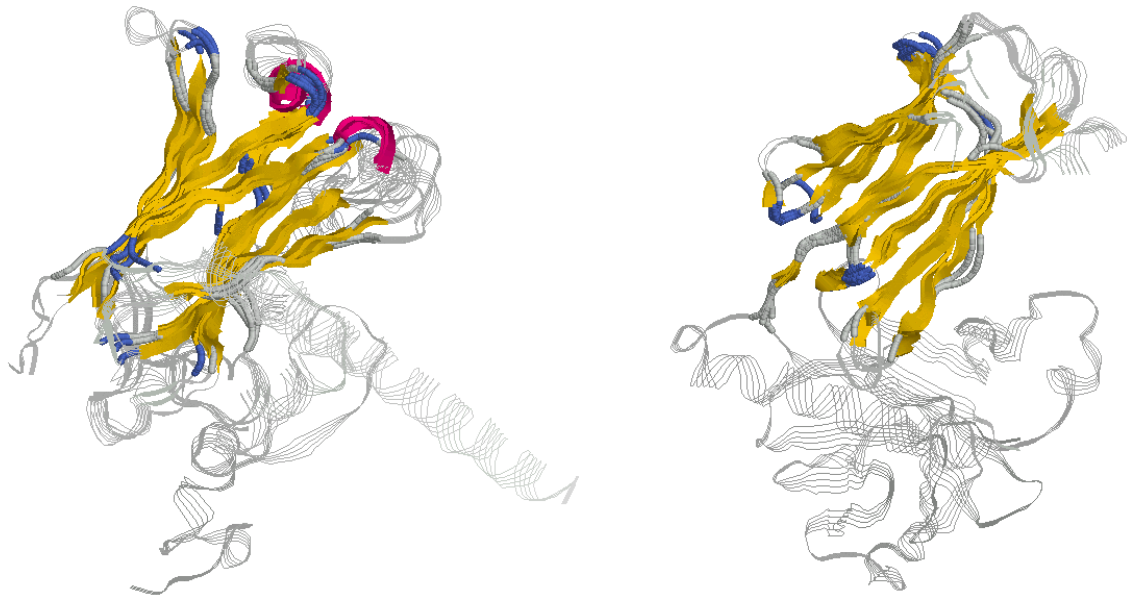

A **B**

Figure 8.

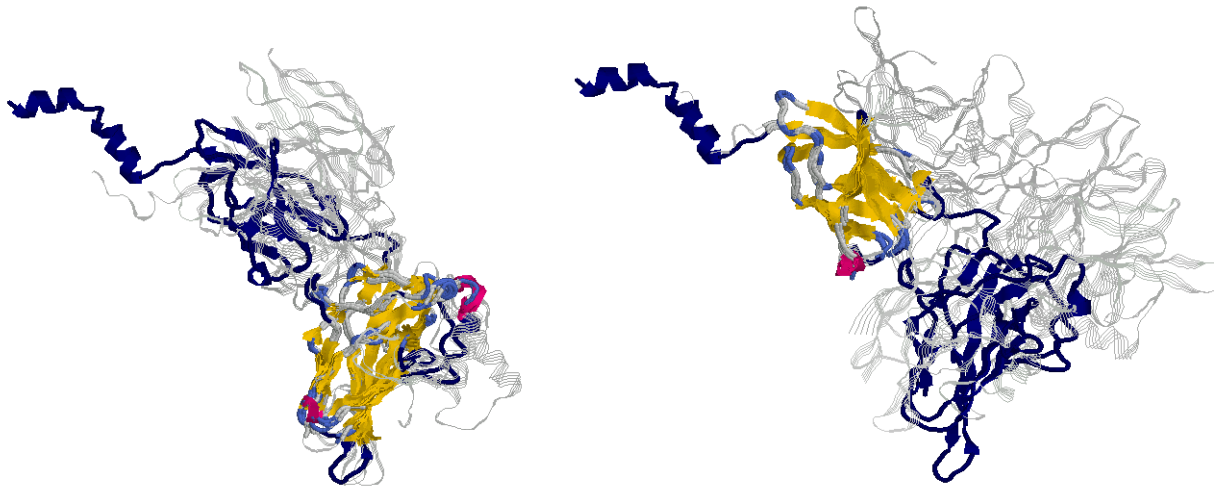

A **B**

Figure 9.

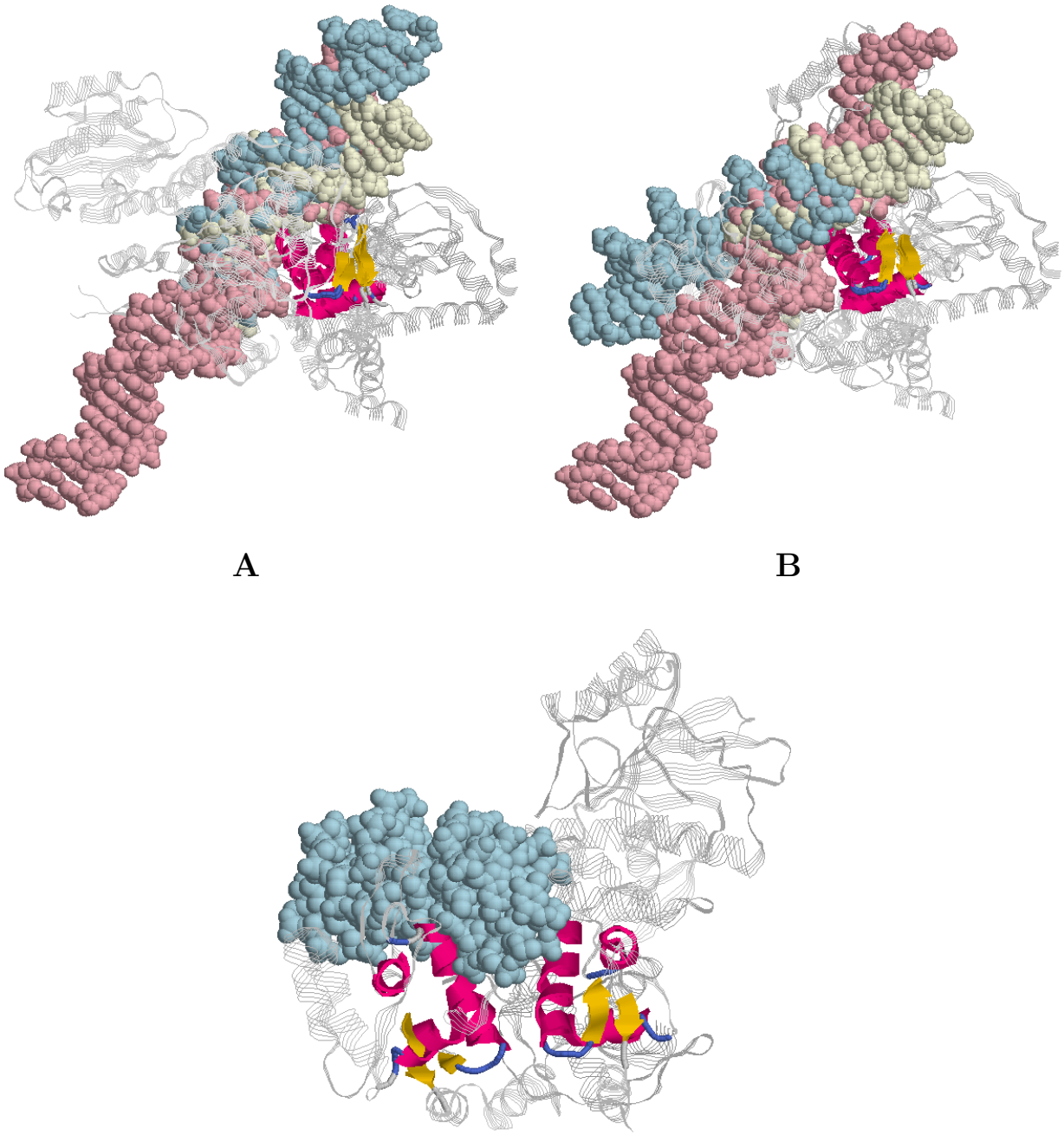

A **B**

C

Figure 10.

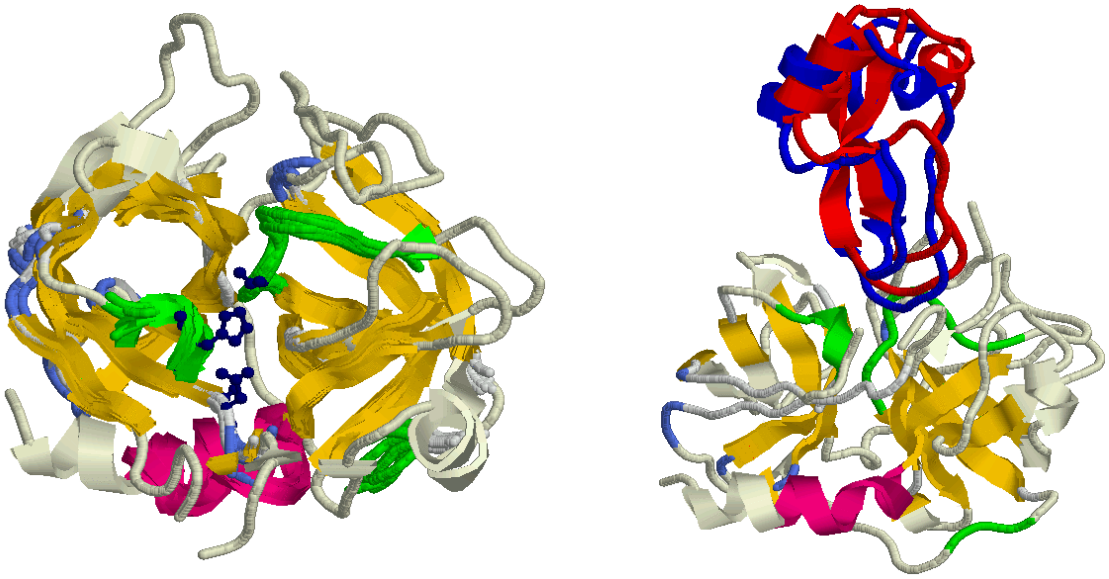

A **B**

Figure 11.